

ANALYSING ANCIENT (VIKING) LONGSHIP STRUCTURES

Reference NO. IJME 1170, DOI: 10.5750/ijme.v164iA2.1170

P R Loscombe, Naval Architect (retired), UK

KEY DATES: Submitted: 04/03/22; Final acceptance: 05/10/22; Published: 30/11/22

SUMMARY

The Nordic longships of the 9th to 11th Centuries were perhaps the preeminent fast assault ships of the period. Modern engineering analytical tools have been employed from time to time to investigate their stability, performance and structural characteristics. The latter is perhaps the most challenging, since the physical problem is that of a hydro-elastic body in rough seas, constructed of a material with highly variable mechanical properties, fastened together by rivets, treenails, nails, spikes, lashings and wedges of uncertain joint efficiency. The corresponding analysis is potentially considerably more complex than the ‘linked-chain’ method commonly employed in modern design offices to establish acceptable scantlings, i.e. classification society rule loads and criteria together with reliable published material property data which are the essential inputs to scantling formulae/finite element analyses (FEA). This paper outlines one small craft naval architect’s view of the issues involved in applying the standard structural design method to the analysis of a ship type which is radically different from modern craft and in so doing identify issues which may be of interest to modern naval architects analysing unconventional lightweight structures. The results may also give a clue as to the possible structural service lives of these ships.

KEYWORDS

Longships, loads, criteria, structural analysis

NOMENCLATURE

B_{OA}	Beam overall [m]
B_{WL}	Beam on waterline [m]
C_B	Block coefficient ($\nabla_c / (L_{WL} \cdot B_{WL} \cdot T_c)$) [-]
C_w	Wave height [m] Bureau Veritas notation
D_c	Canoe body depth at midships [m]
FE	Finite Element
FEA	Finite Element Analysis
FoS	Conventional factor of safety [-]
I_{NA}	Second moment of area of midship section about the neutral axis [m ⁴]
KB	Canoe body vertical centre of buoyancy [m]
KG	Vertical centre of gravity [m]
KM_T	Transverse metacentric height [m]
KN	Righting lever with $KG = 0$ [m]
L_{OA}	Length overall [m]
LOP	Limit of proportionality of wood stress-strain curve [MPa]
L_{WL}	Length on waterline [m]
L_w	$\frac{1}{2} (L_{OA} + L_{WL})$ [m] Bureau Veritas notation
MC	Moisture content = (water mass/oven dry mass) $\times 100$ [%]
SWBM	Still water bending moment [kN.m]
t	Panel thickness [mm]
T_c	Canoe body draft [m]
WBM	Wave bending moment [kN.m]
w_{MAX}	Maximum lateral deflection of panel [mm]
V_k	Ship speed [knots]
∇_c	Volume displaced by canoe body [m ³]
λ	Regular wave length [m]

Wood elastic constants:

E_x, E_y	Elastic modulus in x (parallel to grain) and y (perpendicular to grain) [MPa]
G_{xy}	Inplane shear modulus [MPa]
μ_{xy}	Major Poisson’s ratio

Wood strengths:

MOR	Modulus of Rupture (bending strength of wood) [MPa]
RF	Composite Reserve Strength Factor [-]
X (Y)	Ultimate strength parallel (perpendicular) to the grain respective [MPa]
S	Ultimate strength in shear in the x-y plane

Wood stresses:

$\sigma_x (\sigma_y)$	Direct stress experienced parallel (perpendicular) to grain [MPa]
τ_{xy}	Shear Stress experienced in the x-y plane [MPa]

Classification Societies:

ABS	American Bureau of Shipping
BV	Bureau Veritas
DNV	Det Norske Veritas
LR	Lloyd’s Register of Shipping

1. INTRODUCTION

Ancient or Viking-age “longships” characterised as open-decked, single-mast, clinker-built, largely oak ships are a source of fascination for the amateur enthusiast, including the present author. Numerous websites, semi-technical

publications (e.g. Durham, 2002), public service documentaries and museum exhibits (Williams, 2014) have had a large part to play in raising awareness amongst the general public.

“Longships” have also been a rich vein of research for maritime archaeologists, especially since the unearthing of the two best preserved Viking ships found to date, these being the 24m Gokstad in 1880 and the 22m Oseberg ship in 1904 (Williams, 2014). Around a dozen or so recovered ships, in various states of completeness, are presently located in several European museums as are many more sea-going reconstructions, the latter principally intended for experimental purposes, i.e. testing archaeological hypotheses using real world experience. In the course of this study, the author was able to obtain a glimpse into the world of the maritime archaeologist by reviewing around two dozen open-source papers from specialised journals. These represent only a tiny fraction of the academic database built up over the past hundred plus years; practical constraints limited the number of these which could be consulted in this study.

For obvious reasons, mainly the absence of any commercial incentive, these ancient ships appear only rarely in naval architecture learned journals. Two papers from recent RINA Historic Ship conferences (Handley, 2016, von Ubisch, 2014), a paper from a FAST high speed craft conference (Werenskiold, 2011) and a doctoral thesis (Jensen, 1999) were identified as being amongst the most useful. None of these papers were predominantly focused on structural matters.

Although these ancient Nordic vessels are commonly referred to as longships, the term should generally be reserved for ships carrying numerous warriors intended to be sailed and rowed at speed. They differ from the cargo ship variant by having much higher L_{WL}/B_{WL} , (8-10), higher $L_{WL}/\nabla_c^{1/3}$ (8-11) and higher length:draft ratios.

Longships are also characterised by numerous oar ports typically spaced at around 800-1000mm. Floor/frame spacing appear to reduce with construction date (Crumlin-Pedersen and Olson, 2002). The authors go on to speculate as to whether a figure as low as 700mm for Skudelev 2 – see Table 1 – is really practical as floor spacing equates to the spacing of rowing thwarts. Table 1 shows some estimates extracted from the open literature, arranged chronologically.

This paper is focused on the analysis of a representative ship having structural characteristics closer to those of 11th Century ships rather than those built in the 9th Century (Durham, 2002). In crude terms this means less use of twig lashings to join floors to bottom strakes (i.e. the strakes are left with a pronounced “receiving” clamp on the inside rather than being hewn flush), (von Ubisch, 2014) and a greater use of treenails to join floors and strakes. However

Table 1: Indicative frame spacing.

Ship	Date (approx)	LOA (m) (approx)	Est. Frame Spacing (mm)	Source
Sutton Hoo	625 AD	27 m	914	[a]
Oseberg	820 AD	22 m	1040	[b]
Gokstad	895 AD	24 m	960	[b]
Hedeby 1	985 AD	31 m	840	[b]
Roskilde 6	1025 AD	36 m	780	[c]
Skuldelev 2	1060 AD	29 m	700	[b]

[a] Handley, (2016) - [b] Crumlin-Pedersen, (2014)

[c] Durham, (2002).

coming from a naval architect rather than a marine archaeologist, the foregoing statement should be treated with caution.

A frame spacing of 800mm is adopted which seems to fit with the data given in Table 1. This figure is used for the 3-D FE models as the centre-centre frame spacing and also as the panel short side (fore and aft) in isolated panel studies, notwithstanding the effective short span will be somewhat smaller due to the frame width effect.

2. LIGHTNESS AND FLEXIBILITY

2.1 STRUCTURAL DISTORTIONS

Lightness and flexibility are terms which are frequently used when discussing longship structures (Jensen, 1999). Before commencing any analysis, it is helpful to review distortion data, as reported by crew members, during voyages undertaken by reconstructions. Two examples are paraphrased below;

“VIKING” (1893) – 23.9m (Length overall) × 5.08m (maximum beam) × 1.75m (moulded depth from top of keel).

- keel movement ≈ 20 mm; railings twisted about 157 mm in torsion, gap between lower planks and underside of frames ≈ 16mm (von Ubisch, 2014).

“SEA STALLION” (2008) – 29.3m (Length overall) × 2.9m (maximum beam) × 1.64m (moulded depth from top of keel).

- standing rigging varied from tensioned to completely slack; clinch pins broke, spikes were pulled from joints and wedges were spat out from treenail slots; the whole bow moved 200 to 300mm in a seaway. (Werenskiold, 2011). This latter figure was reported as 500mm in the following website, where a graphic insight into one crew member’s perception of sailing these ships in rough seas may also be found; “It’s like sailing a rubber dinghy that hasn’t been pumped full of air”... (The Viking Ship Museum, (2020).

A modern ship having similar principal dimensions to those of an ancient longship and built of laminated wood (for the sake of argument) would almost certainly be fully

decked. The global bending strength and stiffness would then see an increase of about 280% (see Figure 1). Global strength calculations may not even be necessary and this will almost certainly also be true for the torsional load case. Note Figure 1 is for the 36m L_{OA} case study ship (CS36 – see Section 5) used for illustrative purposes in this paper.

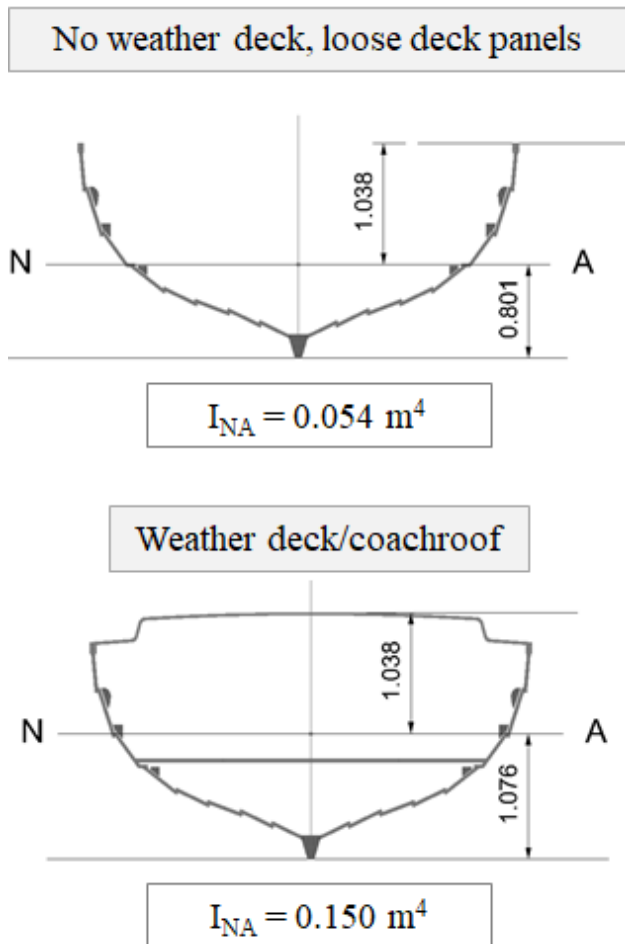


Figure 1. Open-decked v fully-decked midship I_{NA} .

High length to depth ratio, the absence of a weather deck and the use of low-modulus material are essential operational characteristics of the longship so these ships will always be inherently flexible as judged by modern alternatives. These three factors alone may be readily assessed using the standard linked-chain method, either globally or at the local structure level, were it not for two areas of uncertainty;

- The contribution slippage of the mechanical fastenings (if any) makes to global and local flexibility.
- The extent to which structural flexibility causes load reductions compared with those experienced by a modern ship as embodied in class rules.

2.2 FASTENING ISSUES

In modern ship structural analyses, fastenings (welds, glue-lines) are rarely explicitly modelled for anything other than

for assessing structural details. The default starting position is usually linear, shell (2-D) and beam (1-D) FEA. These models have fast run times and no convergence issues and so are ideal for design purposes; many scantlings can be amended merely by altering a few lines of data (e.g. shell thickness, beam cross-section) as opposed to amending the geometry as required in the case of a solid model.

Explicit modelling of the many thousands of mechanical fastenings in a longship is not feasible; it would require a non-linear solid model, with (ideally) three brick elements through the thickness and highly graded meshes in way of the fastenings. Such analyses are much more computationally expensive than linear runs and can take some time to resolve the inevitable convergence issues by trial and error. This would be true for any modern mechanically fastened structure.

In principle it should be possible to evaluate the effect of fastenings at the detail level, provided analyses are informed by idealised physical beam tests, as shown in Figure 2, though such physical tests were not possible here.

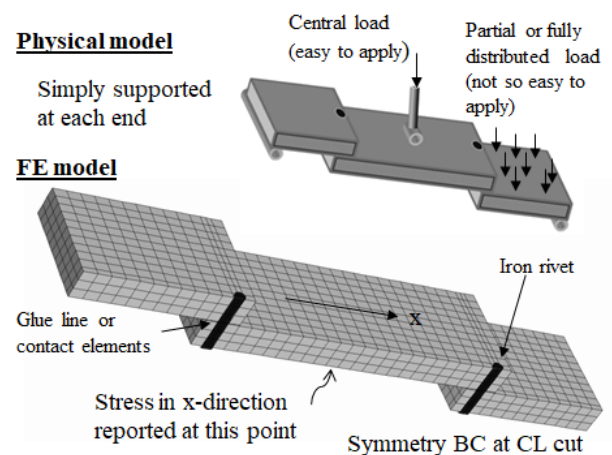


Figure 2. Physical test model and 3-D FE idealisation.

All the FE models reported in this paper were run in Strand7 (Strand7, 2022), in the case of Figure 2, with and without rivets (i.e. “glued”). In the glued beam, a 1mm thick isotropic epoxy glue line pad was modelled and the maximum deflection and a nominal stress were noted. The model was run with both linear and non-linear solvers (but with no contact elements) in order to check that the applied loads were not large enough to introduce any significant geometric non-linearities. It was also run with a 1mm thick wood patch in place of the epoxy pad with very similar results, which confirmed that the glue-line could be ignored, i.e. an all-wood linear FE model would be adequate for nominal stress analyses.

The riveted model was run in the linear mode (i.e. the clamping (pretension) force and contact elements were ignored) and agreed within a percent or two with the glued model. To run in the non-linear mode, assumptions are

required about rivet clamping forces and contact element stiffness. Various assumptions were tried with the result that the nominal stress value was not greatly affected but that deflection increases over the linear glued model were very variable. This very limited study only considered metal riveted joints; the same issues must arise for all the other types, i.e. treenails and friction wedges.

Testing an idealised physical model using bolts as a convenient proxy for rivets would provide insights into the effect pre-tensioning has on overall deflections and if suitably strain-gauged, stresses clear of the joints. However the actual level of clamping force achieved by ancient shipwrights for manually cold-driven bog iron rivets can only be a matter for conjecture; a figure of 25% (of the force to initiate yielding) was suggested as achievable with cold-driven rivets (Deng & Hutchinson, 1998) although this was for joining metal plates.

Even assuming this could be replicated and tested, the spatial distribution and the effect of time would be difficult to ascertain. As an illustration, Section 2.1 talks of wooden rivets spitting wedges out (see website link). One author states that the only way to remove a treenail, once immersion in water has caused the wood to swell, is to drill it out (Gerr, 2000). Perhaps the flexibility of the structure *may* be working the hull to such an extent that normal assumptions are less reliable.

For practical structural calculations, it is only feasible to adopt some simple devices which attempt to account for some loss of stiffness due to the presence of mechanical fastenings.

One approach adopted for the FEA of the support cradle for the museum Swedish warship “Vasa” (Afshar *et al*, 2021) was to use elements without treenails but with reduced elastic moduli. The reduction factor was obtained by matching the maximum deflection of the simplified model to that of a solid FE model which included treenails.

In this paper an ad-hoc approach is adopted; for example, the elastic modulus in the grain direction (E_x) is taken directly from three-point bending tests, uncorrected for shear deflection. This means the inplane modulus is being underestimated by about 10%.

2.3 LOAD ISSUES

2.3 (a) Panel flexibility and local loads

Virtually all classification society rules use the same pressure formulae irrespective of hull material. This question is only relevant to impact loads (bottom slamming, wave slap). Such loads are readily distinguished from sea loads by the inclusion of an area-reduction factor (Allen & Jones, 1978). It is highly likely that the rule approach has been extensively applied to numerous plywood-built craft.

Hence if a representative longship panel is no more flexible than a modern plywood version (designed to the same pressure, boundary condition and appropriate safety factor) then the impact load formulae from class rules should in all likelihood be valid for the purposes of this study.

Table 2 shows a 26mm oak panel of 800×1096 mm subjected to a uniform pressure which just enables it to comply with ABS (2021) using a factor of safety of 2.5. The corresponding pressure was found to be 26 kPa (2.6m static pressure head). The limiting condition for the highly-orthotropic oak panel was strength perpendicular to the grain.

The figure of 800mm is the fore and aft frame spacing (parallel to the grain) and the perpendicular to grain dimension of 1096mm is a reasonable width for four strakes including overlap, although Table 2 applies to carvel plates. Clinker plates are addressed in Section 3.1.

Table 2 shows an equivalent plywood panel which was also designed to just comply with ABS (2021) under the same pressure of 26 kPa with the factor for safety of 2.0 as required for laminated wood. The thickness comes out a little lower, but this time, the limiting condition is strength parallel to the grain. Table 2 shows the plywood panel to be more flexible.

Table 2: Panel comparison; ancient and modern.

800mm x 1096mm, pressure = 26 kPa, fixed edges

All panels are carvel	Mass [kg/m ²]	t [mm]	w _{MAX} [mm]
EUROPEAN OAK			
26mm European Oak (MC = 20%)	19.2	26	2.24
Factor of safety = 2.5 (ABS)	σ _{max} /σ _{allowed} = 0.99 (I to grain)		
PLYWOOD ALTERNATIVE			
15 ply, 600 kg/m ³ PLYWOOD	15.5	24.0	4.09
Factor of safety = 2.0 (ABS)	σ _{max} /σ _{allowed} = 0.99 (// to grain)		

Sheathing for plywood = 1.1 kg/m² No allowance for nails in oak

t = total thickness of plate. w_{MAX} = maximum panel deflection

Oak density at 20% MC = 738 kg/m³ (i.e. 19.2 kg/m²/0.026 m)

This suggests that if impact load formulae from class rules work for modern plywood panels, they should also be reasonably applicable to oak panels.

2.3 (b) Hull flexibility and global loads

While a full hydro-elasticity analysis using integrated computational fluid dynamics and finite element analysis may offer the most complete numerical procedure, this is well outside the remit of this exploratory study. However according to (Haswell, *et al* 2011) hydro-elasticity effects are not considered to be significant when the impact duration/vibration period ratio is greater than two.

For a longship making 9 knots at 60° off the wind in 36m length regular waves (wave period 4.8 seconds), the wave encounter period would be around 3.7 seconds. In

a following sea at 10 knots, the encounter period would be 15 seconds. The fundamental natural period has been estimated to be around 1.13 seconds for CS36 (see Figure 3). In order to elicit a significant hydro-elastic effect, the “impact duration” would need to be less than about 2.26 seconds, i.e. 60% and 15% of the encounter period for 60° and following seas respectively.

This is of course highly speculative but as far as global Load Case 3 (statically poised on a following wave – see Section 7.2(a)) is concerned, it would seem that hydro-elastic effects may be safely ignored at this exploratory stage.

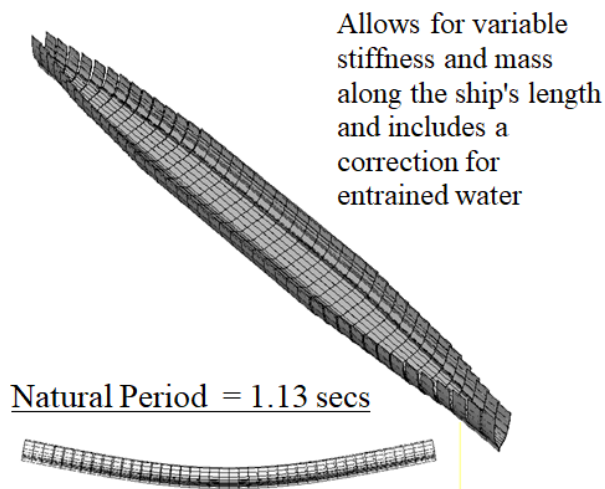


Figure 3. Two-node natural period - FE beam model.

3. FE MODELS

3.1 CLINKER SIMPLIFICATION

Rather than use the nodal offsetting option, a simple “connector” shell is employed at the rivet centre, i.e. at the middle of the overlap zone between adjacent clinker strakes, having the same properties as the strakes. The connector element's thickness (i.e. its width) may be adjusted as required.

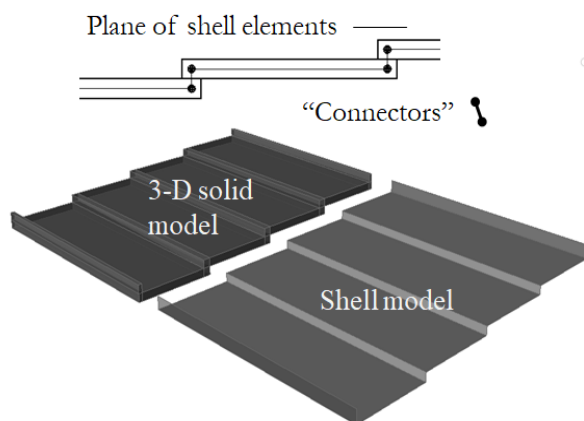


Figure 4. Modelling clinker overlap using 2-D shell.

This width could be the same as the overlap width or a lesser value, empirically adjusted to reflect any relaxation due to the rivet, although as explained in Section 2.2, insufficient data is available to do this at present. The strake width between the rivet centre and the edges is not modelled.

However the real strakes may be convex, not flat as assumed here and would require bevelling of the overlap to mate with the adjacent strake in order to develop the curvature of the transverse sections. These factors are considered less influential in a 2-D shell-based model than the basic shell thickness and can be neglected for exploratory studies of the type discussed in this paper.

As this point in the paper, it is worth pointing out that the precision threshold required for analysis of ancient ships is much lower than that demanded in modern ships. For the latter, the as-built hull will only deviate from the designer supplied hull definition data because of practical manufacturing tolerances. For the former, the hull definition data is the marine archaeologist's best estimate. It is not uncommon when reviewing data for the same ship from different sources to find differences of several centimetres (at least) in principal dimensions. For example, the length overall of the Gokstad is reported as 23.3m (Jensen, 1999), 23.4m (Werenskiold, 2011), 23.8m (Holmes, 1906) and 24.2m (Crumlin-Pedersen, 2014).

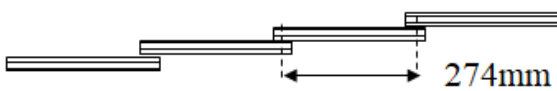
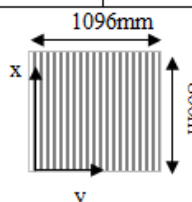
The “connector” shell model idealisation has been checked against a solid model and found to be a little more flexible, which is not unexpected and indeed not undesirable given the likely effect of rivets. The stress agreement is reasonable as shown in Table 3.

An alternative method for idealisation of the clinker shell is to use carvel shell elements with beams to represent the overlap area (Jensen, 1999). This was investigated in this paper using two options; a) a thin web I-beam section with no nodal offset and b) a rectangular beam with nodal offsetting. Deflection and cross-grain direction stress (σ_y) were similar to Table 3 results, although the grain direction stresses (σ_x) were about 30% lower than those obtained using the connector idealisation. The connector method was preferred as it was more suitable for modelling the jogged lower edge of the frames.

Three further points of interest arise from Table 3;

1) As a benchmark, the clinker-built panels have been compared with carvel construction. Both the shell and solid carvel models agree well with an approximate thin-shell orthotropic theory based method (Loscombe, 2017). Deflections aside, the carvel plate stresses are not markedly different from the two clinker plates. This is not surprising as these are maximum stresses which occur at the edges, i.e. clear of the overlap.

Table 3: Validation of overlap idealisation.

ORTHOTROPIC FLAT PANEL; $p = 34.5 \text{ kPa}$, $\text{thk.} = 26 \text{ mm}$, $E_x = 8.528 \text{ GPa}$, $E_y = 1.145 \text{ GPa}$, $G_{xy} = 0.785 \text{ GPa}$, $\nu_{xy} = 0.378$			
800mm x 1096mm; 800mm corresponds to grain (x) direction, 1096mm to cross-grain (y) direction			
			
BUILT-IN	Max stress @ edges		
Source	Defl. [mm]	σ_x [MPa]	σ_y [MPa]
CARVEL PLATE			
CALC. ⁽¹⁾	2.97	16.27	3.99
FE SHELL ⁽²⁾	3.09	16.61	3.96
FEA SOLID ⁽³⁾	3.09	16.67	4.07
CLINKER PLATE			
FE SHELL ⁽²⁾	2.06	19.57	3.42
FEA SOLID ⁽³⁾	1.77	17.02	3.04
(1) Thin shell theory (2) 8-noded thick shell theory (3) 20-noded - 3 solids in thickness direction 12 x 15 mesh for all FE models			

⁽¹⁾ Neglects transverse shear deformation

⁽²⁾ Accounts for transverse shear behaviour
See Cook (1981)

Note; the pressure has been increased to 34.5 kPa in Table 3 from the value of 26 kPa used in Table 2 to reflect design loads evaluated in Section 7. 26 kPa is merely the maximum pressure the carvel 26mm oak panel could withstand and still comply with the ABS safety factor of 2.5.

2) From Table 3 it is possible to calculate the factor of safety for the clinker shell for the case of a 34.5 kPa pressure. Material properties are covered in Section 6 (see Table 5) where the bending strengths parallel and perpendicular to the grain may be seen to be 55.7 MPa and 7.5 MPa respectively. The resulting factors of safety in the two directions are $55.7/19.57 = 2.8$ and $7.5/3.42 = 2.2$. These values will be revisited in Section 9 where for 3-D analysis the presumption of fixed-edges is not required.

3) The stress in the cross-grain direction is 3.42 MPa; if the overlap zone behaved as a very stiff stiffener, so that the panel was effectively reduced to 274mm x 800mm built-in at the edges, the maximum stress in the cross-grain direction (σ_y) would be $0.5 \times 0.0345 \times (274/26)^2 = 1.9$ MPa. Clearly the overlap is not stiff enough for it to be considered as a line of support for this panel setup.

3.2 EXTENDED LOCAL MODEL

A rendered version of the beam and plate model is shown below.

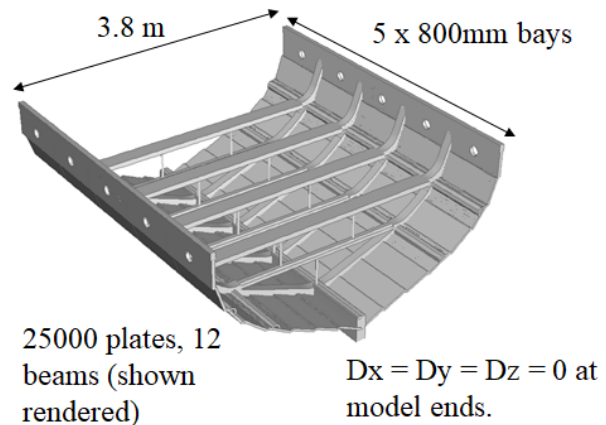


Figure 5. Extended local model.

In any glued idealisation, the shell plating will act as an effective flange to the frames. In traditional plank on frame construction it is common practice to ignore the plate-flange effect due to uncertainties over stress transmission across a nailed or riveted joint (ABS, 2021). In order to bring the FE model into line with the section modulus of the frame in isolation, the frame siding is reduced accordingly.

Longitudinally running elements (strakes, stringers) are aligned by matching the local x and global X directions. This is acceptable as a nominal grain deviation of 5 degrees has been built into the material properties (see Section 6). In the transverse direction, element alignment is done piecemeal by eye in an attempt to make the model more closely reflect the inherent variability of grown frames.

3.3 GLOBAL HULL MODEL

The global model was for a carvel hull. The additional modelling effort of including the connector element approach was not considered to be justified as the stresses of interest are mainly inplane (i.e. primary stresses) rather than secondary or tertiary bending. In any event, Table 3 suggests the error in stresses, even for laterally loaded panels is not excessive.

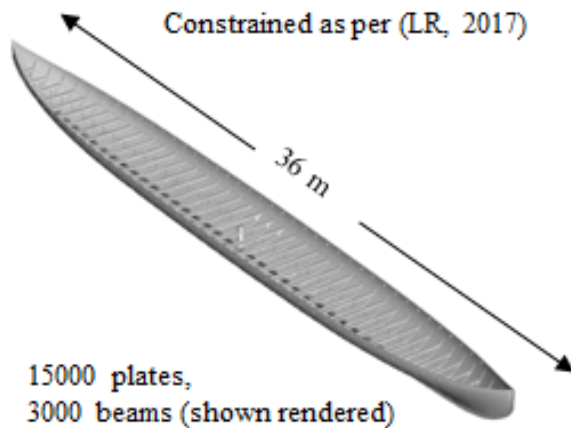


Figure 6. Global hull model.

4. STRENGTH CRITERION

Solid-stock wood is treated as a single ply laminate in the FE analyses used in this study. This provides the option to select from a list of composite Reserve Factor (RF) criteria. Defining wood as an orthotropic material will give the same stresses and deflections but may only allow isotropic criteria such as the von Mises equivalent stress to be selected which is clearly inappropriate for wood. There are several composite failure criteria in use (Gibson, 1994); maximum stress is the simplest of the non-interactive types; Tsai-Hill is the simplest of the interactive type and is preferred here for ease of graphical presentation of results – see Figures 11-14.

The Tsai-Hill based reserve factor is expressed as;

$$R_{TH} = \left[\left(\frac{\sigma_x}{X} \right)^2 - \left(\frac{\sigma_x \sigma_y}{X^2} \right) + \left(\frac{\sigma_y}{Y} \right)^2 + \left(\frac{\tau_{xy}}{S} \right)^2 \right]^{-0.5}$$

where σ_x (X) denote the stress (strength) parallel to the grain, σ_y (Y) denote the stress (strength) perpendicular to the grain and τ_{xy} (S) denote the inplane shear stress (strength). X and Y may be tensile (X_t or Y_t) or compressive strength (X_c or Y_c) depending on the sense of σ_x and σ_y . For analyses where secondary/tertiary (bending stresses) dominate, X and Y are taken as the bending strengths or Modulus of Rupture (MOR) as obtained from a standard three-point bending test using the notation MOR_x and MOR_y , parallel and perpendicular to the grain respectively. For global analyses where primary stresses dominate, the full set of strengths is employed. Note RF has the same meaning as the conventional safety factor (FoS).

The limit of proportionality (LOP) is the point beyond which the structure will be left with permanent set and is often used as a design stress under quite severe loading (see Section 7). Typical LOP values for oak at 20% moisture content (MC) under static bending are 0.53 MOR_x (Depts AF, Navy, Commerce, 1951) and 0.55 MOR_x using regression equations (Forest Products Laboratory, 1989).

5. THE CASE STUDY SHIP CS36M

The case study hull is a 36m (LOA) “paper-ship” loosely based on Skuldelev 2, Roskilde 6 and Hedeby 1 (Crumlin & Olsen, 2002 and Crumlin, 2014).

The scantlings drawn from a synthesis of various sources were as follows; Frame spacing 800mm, shell thickness 26mm, increased to 40mm for the sheer strake; 30mm diameter pillars; 140 (siding) × 80mm (moulding) frames; gunwale rail 80 × 60mm; stringers were idealised as tubes; 200 × 60mm thwart, inverted tee lower deck beams 50 × 30 and 100 × 30. The keel (immersed depth 150mm) and keelson were idealised as a tee section and brackets shapes were taken from various midship section bitmaps obtained from published sources. The mast fish is an indicative idealisation based on photographs.

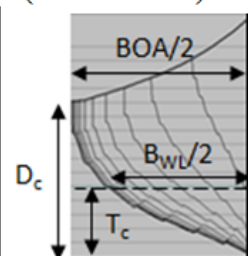
Table 4: Key dimensions and coefficients;

CASE STUDY SHIP "CS36"					
LOA	36.00	BOA	3.80	D_c	1.60
L_{WL}	33.75	B_{WL}	3.12	T_c	0.72
C_B	0.37	C_{WP}	0.73	C_M	0.54
HYDROSTATICS OUTPUT					
WSA	KB	KM_T	Gunwale immersion		
93.8	0.485	2.13	29.6 degrees		

RIGHTING LEVERS (KN) [m] - KG = 0					
ANGLE OF HEEL [degrees]					
5	10	15	20	25	30
0.18	0.37	0.54	0.70	0.86	1.00

WEIGHT BREAKDOWN (ESTIMATED)

Group	Mass/ Δ
Structure	29%
Equipment	4%
Payload	32%
Consumables	6%
Ballast	29%
TOTAL \approx 29 tonnes	



Frames tend to have siding to moulding ratios of 1-2, i.e. much less structurally efficient than modern frames. This was probably a consequence of the method of attachment and the ease of manually bending to fit the curved shell. The frames at 140 × 80 were benchmarked against archaeological data (Crumlin-Pedersen, 2014); at 36m the CS36 was outside the recorded data set, hence the dotted baseline.

For the 140 × 80 fixed-ended frames under a pressure of 34.5 kPa, spaced 800mm apart and spanning about 1100 mm, the maximum stress will be 18.6 MPa corresponding

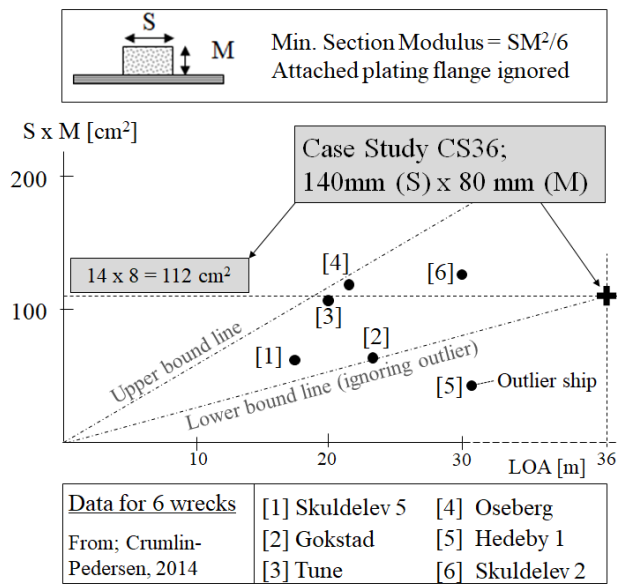


Figure 7. Benchmarking CS36 frame scantlings.

to a factor of safety of 3. This value will be revisited in Section 9.

6. PROPERTIES OF OAK

The most plentiful data is that for clear, straight-grained samples with thicknesses of around 20mm for moisture contents (MC) at both 12% and at the fibre saturation point (often called the “green” condition, typically around 30%) (Risborough, 1974).

Use of these data without corrections would give overly optimistic estimates of mechanical properties; corrections are required for the actual moisture content, log conversion factor (a factor which recognises that nominally cut quarter-sawn strake cross-sections will rarely lie perfectly in the longitudinal-radial plane (L-R)); grain slope variation; statistical variation.

Table 5a shows the formula used for correcting to any moisture content between 12% and the fibre saturation value. Corrections for slope of grain usually employ a Hankinson-type formula (Forest Products Laboratory, 1989).

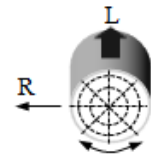
Space does not permit a full explanation of the processes embodied in Table 5a, but standard correction techniques may be found in any text on wood as indicated, e.g. Forest Products Laboratory (1989). Tables 5a and 5b briefly outline the values after each correction, the final results being considered reasonably conservative estimates of material properties for European oak.

Table 5a: Corrected elastic constants.

EUROPEAN OAK

Elastic constant ratios

E_T/E_L	E_R/E_L
0.082	0.154
G_{LT}/E_L	G_{LR}/E_L
0.081	0.089
μ_{LT}	μ_{LR}
0.448	0.350



L = Grain direction

T = Tangential direction

R = Radial direction

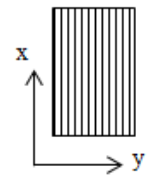
1) WOOD CONVERSION FACTOR

T-R Weighting factor ^a [0.0 to 1.0]

^a 0-0.1 = mainly 'T', 0.9-1.0 = mainly 'R'

E_y/E_x	G_{xy}/E_x	μ_{xy}
0.125	0.086	0.389

0.6



2) CORRECT E_x FOR ACTUAL MC

E_x [MPa] @ 12 % MC	10100
E_x [MPa] @ 27 % MC	8300
E_x [MPa] @ 20 % MC	9102

$n = [12 - M]/[M_{FSP} - 12]$

M_{FSP} = Fibre Saturation Point

$$P_M = P_{12} \left(\frac{P_{12}}{P_G} \right)^n$$

3) CORRECT CONSTANTS FOR GRAIN SLOPE

Grain slope angle			5 deg
E_x	E_y	G_{xy}	
8528	1145	785	
μ_{xy}	G_{RT}	μ_{yx}	
0.378	264	0.051	

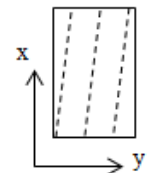


Table 5b: Corrected strengths.

STRENGTH DATA 95% exceedance factor 1.645

Symbol	Mean [MPa]	Std dev [MPa]	De-rated [MPa]	Strength at 20%
MOR_x	97 59	16.8 8.0	69.4 45.8	55.7 MPa
MOR_y	No data; strain taken as 55.7/8528 = 0.65%. $MOR_y = 1145 \times 0.0065$			7.5 MPa
X_c	51.6 27.6	8.0 4.6	38.5 20.0	27.2 MPa
Y_c	9.1 6.2	1.5 1.0	6.6 4.5	5.4 MPa
S	13.7 9.1	2.2 0.9	10.1 7.7	8.8 MPa

97 MPa @ MC = 12%, 59 MPa @ MC = 27%, etc.

Assumption: Tensile strength = Bending strength

7. LOADS

7.1 LOAD LOADS

Local loads obtained from class rules are equivalent static pressures and fall into two categories; sea pressures (hydrostatic pressure in calm water plus the wave effect); impact pressures (load duration is shorter than the wave period), (BV, 2021).

7.1(a) Sea pressures (load case 1)

The waveheight is given in the Bureau Veritas rules (BV, 2021) as $C_w = 10 \log(L_w) - 10$ metres, where C_w is simply denoted as the “wave height” without further clarification and L_w is the wave length defined as the mean of the hull and waterline lengths; for CS36 $C_w = 5.42$ m. The wave pressure at the bottom of the canoe body is 34.5 kPa for the after body, increasing to 47.5 kPa at the bow, presumably to allow for additional pressures due to pitching.

At first sight, a wave height of 5.42m on a wave length of only 34.88m seems excessive given that the theoretical wave maximum height before breaking occurs is about 5m (Comstock, 1967). Conversely in the method used by Lloyd’s Register (LR, 2018), the “wave height” is only 1.87m yet the bottom pressure is similar to the BV value. With a few exceptions it is very difficult to unpick classification society rule formulae; in this case it is impossible to associate any sea state with the specified wave heights, such is the range of possible heights. However a figure of at least 1.5m (significant) would place the ship squarely in sea state 4, “rough sea; moderate waves, many crests break, whitecaps” (Lewandowski, 2004). This is clearly a severe load and linking this with the LOP stress does not sound unreasonable.

Notwithstanding the similarity of BV (2021) and LR (2018) pressures, there is some question as to whether these loads are realistic for a longship.

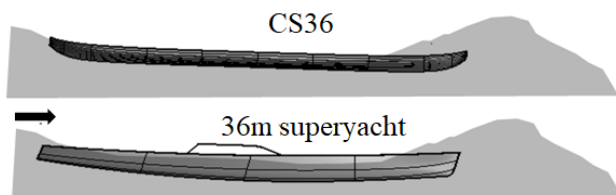


Figure 8. Illustrative “wave-stuffing” load case.

Two ships are imagined to be heading into an oncoming wave front; this is called “wave-stuffing”. For the fully decked superyacht the bow would plough into the steep wave crest which would then break onto the foredeck before running off aft. If the undecked, lower freeboard longship ship were to encounter such a wave, it may be

swamped. There is an inherent danger of capsize due to entrapped water on longships having a large open area, no scuppers and only manual bailing; one account of a swamping event suffered on the Dronningen Queen in 1987 (an Oseberg reconstruction) talks of ship loss in twenty seconds (Paasche *et al*, 2007).

An open-decked ship with no internal subdivision and large numbers on board would find it difficult to fully comply with any modern ship stability criteria. If the gunwale goes under (typically at 20-30 degrees of heel), the ship is likely to be lost. Given this, one might well question whether it is entirely reasonable to adopt loads which are equivalent to a pressure head of twice the hull depth at midships as is the case according to some of the classification society rules which were applied to the CS36. No doubt some dynamic effect is included in the rule formulations. However if one wishes to benchmark these ancient ship structures against modern craft – as is the case in this paper – then there is no option but to apply modern scantling rules in their entirety.

7.1(b) Impact loads (load case 2)

The BV (2021) rule defines two types of impact load; bottom slamming and topside wave slap. These two loads are assumed to occur simultaneously (only for the purposes of this study) at the centre of the middle bay as shown in Figure 9.

The formula may be presumed to apply primarily to modern yacht hulls, i.e. those with moderate deadrise aft, a transom stern and a moderate length:beam ratio, all of which are features which improve the chance of semi-planing and hence increasing accelerations. Bottom slamming is generally worst in the head sea condition, but the reduction in acceleration at say 40 degrees off the wind may not be so large as to invalidate traditional well-known Savitsky-based class rule acceleration formulae.

These features are not to be found in a typical longship. Furthermore, the BV bottom slam pressure corresponds to a $V_k/\sqrt{L_{WL}}$ of 2.7 or 15.7 knots for the CS36. The CS36 close-hauled at around 60° is unlikely to make 15.7 knots at this heading.

Fortunately these matters need not be pursued here, since the objective was to set an outlier longship (in terms of slenderness parameters) a severe test by combining lower-bound scantlings and material properties with upper-bound loads. The same is true of the global loads discussed in Section 7.2. The time to revisit these issues would be only after the corresponding nominal reserve factors have been determined.

The load cases applied to the extended local model are shown in Figure 9.

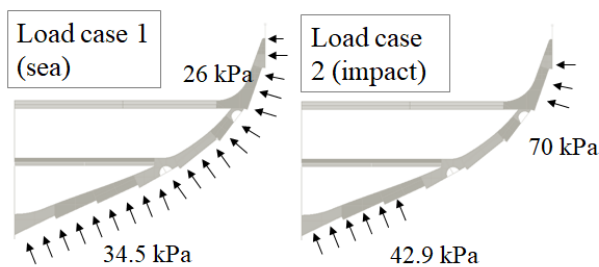


Figure 9. Assessment pressures - load cases 1 and 2.

7.2 GLOBAL LOADS

7.2(a) SWBM + WBM + Rig (load case 3)

By tradition, the ship is assumed to be statically poised on a stationary regular wave and this is still used today at the initial design stage. Although the idea of a ship sitting on a fixed wave is somewhat incongruous at first thought, for a longship this is quite a sound proposition. In regular waves, the wave profile advances at a speed of $2.43 \sqrt{\lambda}$ knots, where λ is the wavelength (i.e. 14 knots for the CS36). The ship itself may be making 12 knots downwind. In other words, the wave overtakes the ship, but only very slowly.

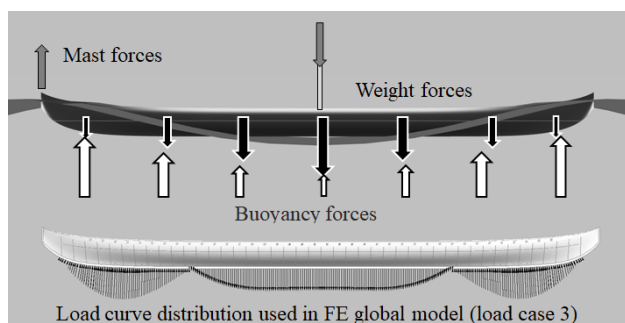


Figure 10. Ship statically-poised on a following wave.

The worst case sagging load corresponds to a wave crest at the aft and forward ends of the ship, the concentration of stone ballast blocks as close to midships as the stowage rate permits (taken here as $0.6 \text{ m}^3/\text{tonne}$ for rounded granite blocks) and including the rig load. Hull girder sagging will place the sheer strake into compression. The load (weight-buoyancy) is applied as vertical edge pressures distributed along the underside of the keel as shown in Figure 10.

7.2(b) Rig induced bending

Hemp is the modern cordage used for the standing rigging on reconstructions and since few examples of rigging have survived the ravages of time, these replica rigs have been presumably dimensioned using a modern method such as the Nordic Boat Standard (NBS), (Larsson *et al*, 2014). This was used in this study to estimate the required rigging diameter for the Roar Ege (Skuldelev 3 reconstruction). The resulting figures of 28mm (fore and back stay) and

20mm (shrouds) compared well with published figures of 20-26mm for the actual Roar Ege (Crumlin-Pedersen, 2014).

Repeating the exercise for the CS36 resulted in hemp diameters of 40mm (fore and back stay), 29mm (shrouds). Lime bast appears to be one of the options used by ancient riggers. Limited data suggested an ultimate strength value of 21 MPa (Myking, *et al* 2005) which compares with 77 MPa used to dimension the standing rigging in hemp. The revised dimensions in lime bast are therefore $(77/21)^{1/2} \approx 2$ times the hemp values, which begs questions as to the practicality of handling 80mm and 60mm diameter cordage.

With this uncertainty, the normal rule approach of using 40% of breaking load as the basis for determining the rig-induced bending moment was abandoned. Instead the moment was based on the drive force in an assumed downwind sailing condition of 10 knots under full sail (136 m^2) in gusting Force 7 (33 knots). The sail drive force was partitioned between mast head and sheets and the rig load was applied as a vertical force (up) of 7 kN at the back stay chain plate and a vertical force (down) of 7 kN at the mast; the horizontal component of the stay tension being ignored.

7.2 (c) Torsion – global load case 2

Two methods were evaluated; a large ship classification society formula and a worst-case grounding scenario. The DNV formula (DNV, 2017) was used in an earlier study (Jensen, 1999) but has since been updated to a fully dimensionally consistent format; the maximum torque for CS36 was found to be 108 kN.m. For the grounding case, the 29 tonne CS36 is imagined to be aground and then left ‘high and dry’ by the tide, only supported at two points, one rock to port, the other to starboard. Assuming each rock is located at 25% of the waterline beam off the centreline, the maximum torque would be 114 kN.m

8. RESULTS

8.1 INTERPRETATION OF STRESS PLOTS

FE stress plots as presented in technical papers can be difficult for readers to examine rigorously due to their complexity, compounded by the reduced scale. Only four key plots are presented here but these are sufficient to indicate how the CS36 fares under the loads described in Section 7.

Each plot shows just four RF contours (of which only three are present);

- Inadequate scantlings, i.e. risk of failure, RF is less than 1.0 (no failure zones were identified)
- Light scantlings (LOP exceeded); RF is greater than 1.0 but less than 2.2

- Adequate scantlings (LOP not exceeded); RF is greater than 2.2 but less than 4.0
- Scantlings in line with BV rules; $RF > 4.0$

The RF limits:

The value of 2.2 is obtained from $1/(0.53 \times 0.85)$; 0.53 comes from Section 4; 0.85 is a scantling manufacturing tolerance factor.

A representative value for this factor was based on an assumed $\pm 2\text{mm}$ tolerance on a 26mm strake, bearing in mind all components are hand-cut and presumably sized by rudimentary methods; 0.85 is obtained from $(24/26)^2$. This may be compared with the ABS (2021) safety factor of 2.5.

As the loads are based on the Bureau Veritas (2021) rule, it is appropriate to include the associated BV safety factor of 4. The zones are identified by arrows in Figures 11 to 14.

It should be mentioned that the data in Tables 5a and 5b were taken from tests on clear, straight grained specimens, typically around 20mm thick. This is reasonable for planking. However there is a size effect on wood mechanical properties; the deeper the section, the greater the likelihood of strength reducing defects, such as knots. The data in Tables 5a and 5b may be non-conservative for 100- 150mm deep components. However this factor is ignored in this study.

8.2 RESULTS - LOCAL MODEL

All presented stresses are *nominal* values, i.e. overestimates for areas stressed above the limit of proportionality (due to using a linear material model) and unable to identify the very steep stress gradients which might be expected around rivet holes and the like.

Tsai-Hill strength reserve factors are shown for load cases 1 and 2 in Figures 11 and 12.

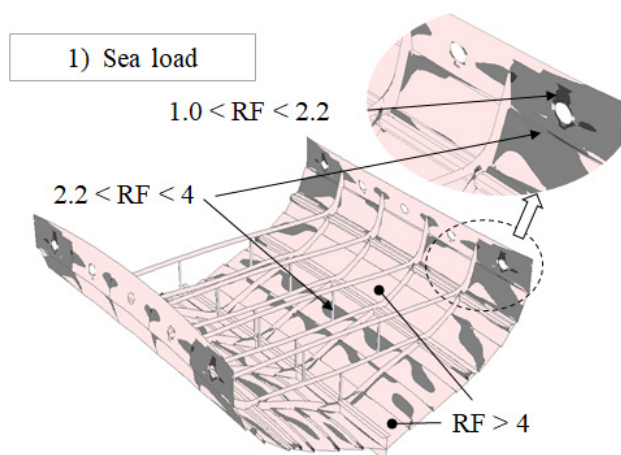


Figure 11. Tsai-Hill RF (load case 1).

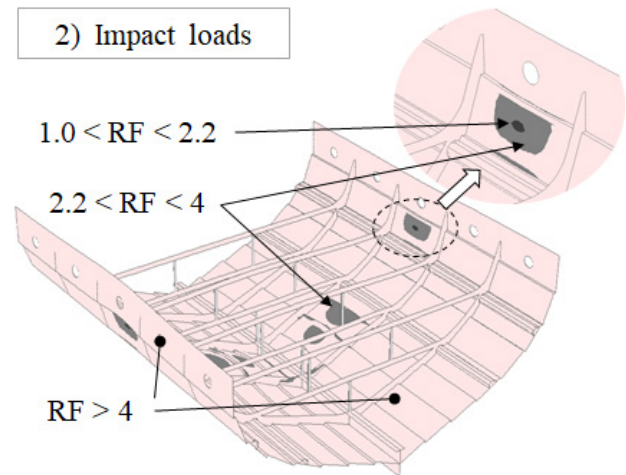


Figure 12. Tsai-Hill RF (load case 2).

8.3 GLOBAL MODEL

Tsai-Hill strength reserve factors are shown for the two global load cases;

Load case 3 – Still water + wave + rig induced vertical bending moments
See Figure 13.

Load case 4 – Torsional load
See Figure 14

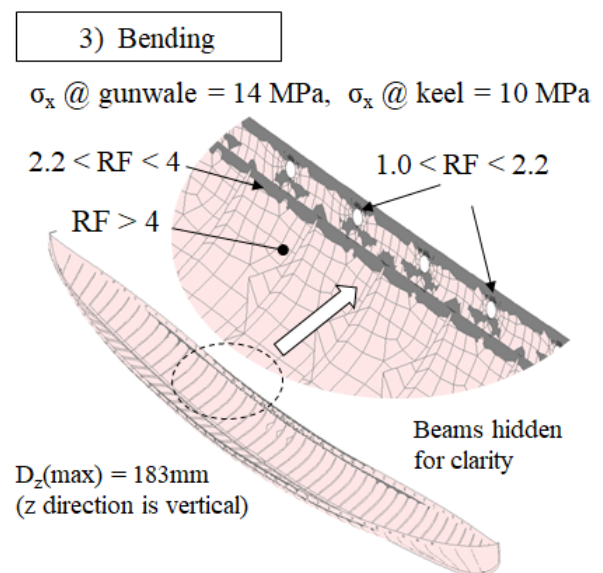


Figure 13. Tsai-Hill RF (load case 3).

9. ANALYSES OUTCOMES

Figures 11 to 14 show the same RF pattern; the vast majority of the structure has RF values which exceed the BV factor of safety of 4. Of the more highly stressed zones, most lie in the 2.2 to 4 range with only a very few highly

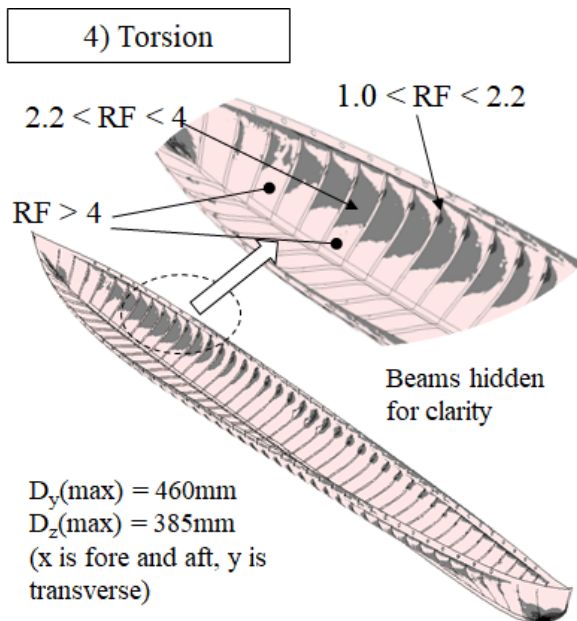


Figure 14. Tsai-Hill RF (load case 4).

localised zones having RF in the 1.0 to 2.2 range. There are no areas indicating failure ($RF < 1$).

Figures 11 and 12 are in line with the simple hand calculated factors of safety described earlier; for the clinker panel = 2.2 (see Section 3.1); for the 140 x 80mm bottom frame = 3.0 (Section 5).

Figure 13 stresses are in line with simple hand calculations and FE beam model results. The BV rule total bending moment (868kN.m) is used with the midship section data from Figure 1 to give primary stresses of 16.8 MPa (gunwale) 13.0 MPa (keel). The 26-segment beam-element model (see Figure 3) was subjected to same load as applied to the full FE global model (see Figure 10). The resulting primary stresses were 17.7 MPa (gunwale) 13.8 MPa (keel) with a maximum deflection of 205mm. The corresponding values in Figure 13 are 14 MPa, 10 MPa and 183mm respectively.

The hull under torsion has larger areas in $2.2 < RF < 4$ category compared with bending, but this might be in part due to the way the load is applied, as shown in Figure 15.

This approach is similar to that used in container ships where the vertical forces are applied through the side shell. As the CS36 is undecked, this may be causing some unrealistic local effects. Some additional knees were added here and other methods of applying the torque forces were tried with little effect on RF distributions. It may be that a more sophisticated load distribution algorithm is required.

The global distortions of 0.18m to 0.5m are of the same order as those reported by crew members on reconstruction ships (see Section 2.1), although comparing a static 'dry' FE model with a real ship in a seaway is not very meaningful.

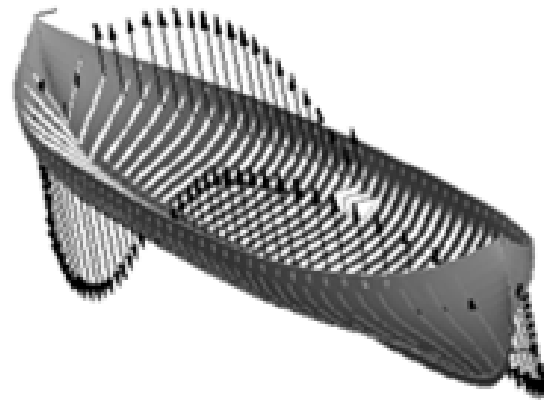


Figure 15. Opposing torque forces applied at thwarts.

As mentioned in Section 7.1 (b), this preliminary study should be considered as representing a fairly severe test of the longship structure. Despite this, most parts of the ship would appear to stand a reasonable chance of complying with modern classification society requirements. If confirmed by subsequent investigations, this is a testament to the intuitively based skills of the ancient shipwrights who created them.

One caveat must be added to the foregoing; all the analyses are for nominal stresses. The various mechanical fastenings (not modelled) may well cause stress concentration factors that could exceed the standard isotropic material factor of around 3, particularly as degradation and movement of the initially hot-dipped rivet may well cause substantial erosion of the wooden rivet-hole. This is beyond the scope of this paper but it is entirely possible that a nominal reserve factor of 4 may not be as conservative as may first appear.

10. CONCLUSIONS

This study was undertaken for reasons of pure academic curiosity. There was no commercial element or any external funding involved. The principal objective was to estimate likely nominal stress levels experienced by these ancient ships in service using standard structural design methods.

The paper explains why explicit inclusion of mechanical fastenings into structural models would raise the level of analytical complexity to a point well beyond the capabilities of standard design methods and certainly the resources available to the author.

The paper discusses a number of uncertainties on load prediction and material properties and describes how conservative values have been obtained for both which reflect the differences between longships and modern craft, as far as that is possible.

The paper also explains that structural failures must be seen in the context of a ship whose essential characteristics

make it extremely vulnerable to loss through swamping/instability, at least compared with modern vessels.

A lower data accuracy threshold has been adopted for this study than would be acceptable with modern ship design where lives are at stake. This was partly enforced by the paucity of open-source data, but is also an inherent characteristic of ancient ships analyses. The Gokstad and Oseberg ships apart, most finds are restricted to the lower reaches of the hull – see website showing the state of the recovered hulls for the Skuldelev ships (The Viking Ship Museum, 2008) – and hence considerable uncertainty must exist over the original as-built structural configuration and scantlings.

Structural analyses have been conducted on a case study ship deliberately processing characteristics likely to exacerbate structural problems, for example high length:depth ratio, degraded mechanical properties (high moisture content, statistically de-rated) and lower-bound scantlings. Despite this, it appears that most parts of the ship would stand a reasonable chance of complying with modern classification society requirements. One might argue that if ancient longships strength reserve factors are not dissimilar to those of modern craft, the structural service life of the former may be similar to that of the latter, i.e. decades, not just a dozen or so cross North Sea raids.

At this time it is the author's contention that the type of simplified, cost and time-efficient structural assessment procedures discussed within have a part to play in hypothesis-testing which might complement standard archaeological methodologies.

11. FUTURE WORK

It is recommended that additional engineering studies (of the type described in this paper) should be conducted as they might shed further light on the structural behaviour of these interesting ships at minimal cost/resource. Even if the substantial funding required to support more computational and experimental resource-intensive research is available, it makes sense to do these types of analyses as a precursor.

It would be worth combining local and global loads, even linearly. However, this is not a trivial task as applying the global load as a distributed local pressure load requires some consideration. A step-up in complexity would be to run the resulting model as a non-linear analysis in order to identify any beam-column magnification effects.

Modern sailing craft are rarely lost due to gross structural failure of the hull; loss of keel, rudders and mast may be more likely initiators. It would not be difficult to conduct "design-office" level investigations into the strength of steer boards and masts using conventional methods. Indeed, modern load algorithms may be used with more confidence for these components. The studies would be

further enhanced if material tests on rudder fasteners and standing rigging could be included as well as FEA and testing of ancient shroud pins. This would make an unusual and interesting graduate project.

Another interesting question which often comes up when reading about longships is 'does the flexibility of the hull girder reduce loads', i.e. as compared with the rigid-hull assumption used in most design-office procedures? Section 2.3 (b) has made a stab at this but a semi-empirical approach would be much more convincing.

One pragmatic approach would be to instrument one of the larger, more slender ship reconstructions with accelerometers, say at the bow, midships and at the stern and conduct sea trials in moderate seas at say 60 degrees off the wind. This would endanger neither the ship nor its crew. A modest data record would be sufficient to give reliable heave and pitch significant accelerations. The impact of fasteners and material/geometry on hull girder stiffness is automatically included with this approach.

Such a sailing condition would fit nicely within the limitations of conventional frequency-domain based seakeeping software (i.e. design office level). Comparing strip theory's theoretical rigid body accelerations with measured values might yield a clue to this question at only modest cost and effort.

12. REFERENCES

1. ABS (2021). *Guide for building and classing Yachts*. Part 3 Hull Construction and Equipment. American Bureau of Shipping. Houston, Texas, USA.
2. AFSHAR, R., ALAVYOON, N., Ahlgren, A. and Gamstedt, E. K. (2021) *Full scale finite element modelling and analysis of the 17th Century warship Vasa: A methodological approach and preliminary results*. Engineering Structures. 231. doi.org/10.1016/j.engstrut.2020.111765.
3. Allen R.G. and Jones R.R. (1978). *A simplified method for determining structural design limit pressures on high performance marine vehicles*. Proceedings of the IAA/SNAME Advanced Marine Vehicle Conference (April 1978). San Diego, CA, USA.
4. BV - Bureau Veritas (2021) *Rules for the classification and the certification of yachts*. NR 500 DT R00 E. Paris, France.
5. COMSTOCK, J. P. (1967) *Principles of naval architecture*. Society of Naval Architects and Marine Engineers. Alexandria, Virginia, USA.
6. COOK, R. D. (1981) *Concepts and applications of finite element analysis*. John Wiley & Sons, Inc. ISBN 0-471-87714-X. New York, NY.
7. CRUMLIN-PEDERSEN, O. (2014) *Viking-age ships and shipbuilding in Hedeby/Haithabu and*

- Schleswig*. 2nd impression. Ships and Boats of the North, Vol.2. The Viking Ship Museum, Roskilde. Denmark. ISBN 87-85180-30-0.
8. CRUMLIN-PEDERSEN, O. and Olsen, O. (2002) *The Skuldelev Ships I*. Ships and boats of the North, Vol.4.1. The Viking Ship Museum, Roskilde. Denmark. ISBN 87-85180-467.
9. DENG, X and HUTCHINSON, W (1998) *The clamping stress in a cold-driven rivet*. Int. J. Mech, Sci, Vol 40, No.7.
10. DEPARTMENTS OF THE AIR FORCE, NAVY and COMMENCE (UNITED STATES) (1951). *Design of wood aircraft structures*. 2nd Ed. ANC-18 Bulletin. Prepared by the Forest Products laboratory, Wisconsin, USA.
11. DNV (2017) *Rules for classification – ships. Part 3. Chapter 4 (loads), section 4 (hull girder loads), 3.4 (wave torsional moment)*. Ed Jan 2017. Høvik, Norway.
12. DURHAM, K. (2002). *Viking Longship*. Osprey Publishing. Oxford, UK. ISBN 1 841763497.
13. FOREST PRODUCTS LABORATORY (1989) *The encyclopedia of wood*. Revised Edition, Sterling Publishing Co. New York, NY, ISBN 0-8069-6994-6 (1989)
14. GERR, D. (2000) *The elements of boat strength*. Adlard Coles Nautical, London. ISBN 0-7136-5751-0.
15. GIBSON, R. F. (1994) *Principles of Composite Material Mechanics*. McGraw-Hill International Ed. New York, NY. ISBN 0-07-113335-6.
16. HANDLEY, P. (2016) *The Sutton Hoo Saxon ship – development and analysis of a computer hull model prior to full scale reconstruction*. RINA Historic Ships, 7-8 December 2016, London.
17. HASWELL, P.K., WILSON, P.A., TAUNTON, D.J. and AUSTEN, S. (2011) *Design and performance of inflatable boats: flexibility and environmental considerations*. High Speed Marine Vehicles (HSMV 11), Napoli, Italy. Royal Institution of Naval Architects.
18. HOLMES, G. C. V (1906) *Ancient and modern ships. Part 4 Wooden sailing ships*. Her Majesty's Stationary Office. London.
19. JENSEN, K. (1999) *Documentation and analysis of ancient ships*. PhD thesis, Centre for Maritime Archaeology, Department of Naval Architecture and Offshore Engineering, Technical University of Denmark. Lyngby.
20. LARSSON, L, ELIASSON, R. E. AND ORYCH, M. (2014) *Principles of yacht design*. 4th Ed. 4. Adlard Coles Nautical, London. ISBN 978-1-4081-8790-6.2014.
21. LEWANDOWSKI, E. M. (2004) *The dynamics of marine craft – maneuvering and seakeeping*. World Scientific Pub. Singapore. ISBN 981-02-4755-9.
22. LOSCOMBE, P. R. (2017) *Taking the simple measures of laminates*. Professional Boat Builder, No. 166 (April/May), p.31.
23. LLOYD'S REGISTER (2017) *ShipRight design & construction, structural design assessment, primary structure of container ships*. Lloyd's Register of Shipping, London.
24. LLOYD'S REGISTER (2018) *Rules and regulations for the classification of special service craft*. Lloyd's Register of Shipping, London.
25. MYKING, T., HERTZBERG, A (2005) and SKOPPE, T (2005) *History, manufacture and properties of lime bast cordage in northern Europe*. Forestry, Vol. 78, doi:10.1093/forestry/cpi006.
26. PAASCHE, K. RØVIK, G. AND BISCHOFF, V. (2007) *Rekonstruksjon av Osebergskipets form – rapport fra Osebergprosjektet 2006*. (in Danish/Norwegian) Oslo, Roskilde, Tønsberg, 18.12.2007.
27. RISBOROUGH (1974) *Strength properties of timber*. Princes Risborough Laboratory, the Building Research Establishment), Published by MTP Construction. Lancaster, UK. ISBN-10 : 0904406253
28. STRAND7 (2022). Finite element analysis software. <https://strand7.com>. (Accessed 8th March 2022)
29. VON UBISCH, B. (2014) *The building and the journey of the Viking ship "Viking" in 1892-1893*. RINA Conference on Historic Ships, London 2014.
30. WERENSKIOLD, P. (2011) *The most sophisticated and successful high-speed ships for their time*. 11th International Conference on Fast Sea Transportation, FAST 2011. Honolulu, Hawaii, 2011.
31. WILLIAMS, G. (2014) *The Viking ship'* The British Museum Press, London. ISBN 978-0-7141-2340-02014
32. VIKING SHIP MUSEUM (2008) *Heavy seas and flexibility*, Roskilde, Denmark. (Accessed 18th December 2021) <https://www.vikingskibsmuseet.dk/en/about-us/subscribe-newsletter/newsletters/sea-stallion/newsletter-39-issue-16-august-2008>,
33. VIKING SHIP MUSEUM (2022) *The five Viking ships*, Roskilde, Denmark (Accessed 10th January 2022) <https://www.vikingskibsmuseet.dk/en/visit-the-museum/exhibitions/the-five-viking-ships>.